International Journal of General Medicine

Dovepress
Taylor & Francis Group

Open Access Full Text Article

ORIGINAL RESEARCH

Integration of Bulk and Single-Cell RNA Sequencing to Identify RNA Modifications-Related Prognostic Signature in Ovarian Cancer

Shaoyu Wang[1–3], Qiaomei Zheng[1–3], Lihong Chen[1–3]

[1]Department of Obstetrics and Gynecology, The First Affiliated Hospital, Fujian Medical University, Fuzhou, 350005, People's Republic of China; [2]Department of Obstetrics and Gynecology, National Regional Medical Center, Binhai Campus of The First Affiliated Hospital, Fujian Medical University, Fuzhou, 350212, People's Republic of China; [3]Fujian Key Laboratory of Precision Medicine for Cancer, The First Affiliated Hospital, Fujian Medical University, Fuzhou, 350005, People's Republic of China

Correspondence: Lihong Chen, Email wscclh@163.com

Background: Ovarian cancer (OC), a common fatal malignancy in women, has a poor prognosis. RNA modifications are associated with the development of OC. In this study, we aimed to identify and verify RNA modifications-related prognostic genes in OC by integrating bulk and single-cell RNA sequencing (scRNA-seq) data.

Methods: Transcriptome data came from public databases and RNA modifications-related genes (RMRGs) were obtained from literature. Candidate genes were identified by intersecting RMRGs with differentially expressed genes (DEGs) in OC patients. Prognostic genes were gained via machine learning techniques, particularly LASSO regression. A risk model was built to predict the prognosis. OC patients were divided into high-risk and low-risk groups according to risk score. Subsequent analyses covered enrichment analysis, immune microenvironment, mutation analysis, and chemotherapeutic drug sensitivity. In addition, scRNA-seq data was assessed for key cells and gene expression in them. Finally, RT-qPCR was applied to identify the expression of prognostic genes.

Results: *LSM4, SNRPC, ZC3H13, LSM2, WTAP, DCP2, PUS7*, and *TUT1* were selected as prognostic genes. The risk model exhibited excellent predictive abilities. Seventeen pathways were enriched like calcium signaling pathway, 7 differential immune cells were identified like regulatory T cells and plasmacytoid dendritic cells, and *TP53* had highest mutation rate. Half-maximal inhibitory concentrations (IC50) values of 47 drugs like paclitaxel differed between two risk groups. The prognostic genes were distributed mainly in fibroblast cells, epithelial cells and endothelial cells. During fibroblast cells differentiation, expression of prognostic genes fluctuated to varying degrees. The RT-qPCR demonstrated that the expression of *LSM2, LSM4, PUS7, SNRPC*, and *TUT1* were upregulated in OC, while *DCP2, WTAP*, and *ZC3H13* were downregulated.

Conclusion: We constructed an RNA modifications-related prognostic signature that can effectively predict clinical outcomes and therapeutic responses in patients with OC.

Keywords: ovarian cancer, RNA modifications, single-cell RNA sequencing, immune microenvironment, prognostic genes

Introduction

Ovarian cancer (OC) has the highest mortality rate among gynecological malignant tumors. Owing to the lack of early specific symptoms, sensitive screening and diagnostic biomarkers, more than 70% of patients are diagnosed at an advanced stage. The standard treatment for OC includes cytoreductive surgery, platinum-based chemotherapy, and targeted therapy.[1] Although immunotherapy has advanced in other cancers, its efficacy in OC remains limited. The majority of patients eventually relapse because of the high tumor heterogeneity and inherent or acquired therapy resistance associated with the complex tumor microenvironment (TME).[2,3] These challenges underscore the urgent need for reliable prognostic models and novel biomarkers to stratify high-risk patients and guide personalized interventions.

Received: 16 March 2025
Accepted: 15 May 2025
Published: 20 May 2025

To address these issues, targeting epigenetic regulators like RNA modifications has emerged as a promising strategy. There are a lot of chemical modifications on the bases and ribose of coding RNA (message RNA, mRNA) and most non-coding RNAs. More than 170 different types of post-transcriptional modifications have been identified in RNA, including N6-methyladenosine (m6A), N1-methyladenosine (m1A), 5-methylcytidine (m5C), N7-methylguanosine (m7G), 2′-O-methylation (2′-O-Me), pseudouridine (Ψ), adenosine-to-inosine (A-to-I) editing and uridylation. These modifications can be deposited, removed and recognized in a reversible way by corresponding enzymes (writer, eraser and reader).[4] RNA modifications have been confirmed to participate in the pathogenesis of OC. These modifications affect RNA splicing, stability, translation, and interactions between RNAs, thus regulating the expression of oncogenes or tumor suppressor genes.[5] For example, the m6A methyltransferase METTL3 promoted the maturation of miR-126-5p to upregulate PTEN and thus activated the PI3K/Akt/mTOR pathway to promote OC progression.[6] The RNA methyltransferase NSUN2 facilitated E2F1 mRNA m5C modification and formed a positive feedback regulatory loop to upregulate E2F1 expression, driving OC progression.[7] However, the functional heterogeneity of RNA modifications across OC cell subsets remains elusive, limiting their clinical utility.

Traditional bulk RNA sequencing (RNA-seq) combines large amounts of subsets cells and shows average expression level, which ignores the extensive intra-tumor heterogeneity among tumor cells. Single-cell RNA sequencing (scRNA-seq) uses next-generation sequencing methods to analyze the transcriptome at the cellular level. This method can assess intra-tumor heterogeneity, delineate different cell subsets and their functional status.[8] By integrating bulk RNA-seq and scRNA-seq data, we can explore genetic and functional heterogeneity on the basis of maximizing the discovery of differentially expressed genes (DEGs), leading to a better understanding of the pathogenesis of OC.

Therefore, we aimed to construct and validate an RNA modifications-related prognostic signature for OC patients based on bulk RNA-seq and scRNA-seq datasets. In this study, we first identified DEGs related to RNA modifications in OC patients. A prognostic risk model was constructed by utilizing machine learning algorithms. Subsequent analyses on high-risk and low-risk groups covered enrichment analysis, immune microenvironment, mutation analysis, and chemotherapeutic drug sensitivity. Moreover, scRNA-seq data was utilized to determine the expression of prognostic genes in key cells. Finally, we validated the prognostic gene expression in human OC tissues compared with that in tumor-adjacent tissues. Our results may provide new biomarkers for evaluating the prognosis of OC patients and provide new insights for further research on the role of RNA modifications in OC progression.

Materials and Methods

Data Acquisition

The flow chart of our study is presented in Figure 1. The Cancer Genome Atlas-Ovarian Cancer (TCGA-OV) dataset containing 400 OC tissue samples with survival information was downloaded from University of California, Santa Cruz (UCSC) Xena (https://xena.ucsc.edu/), and was applied as training set. The GSE26712 (GPL96), GSE23554 (GPL96), and GSE184880 (GPL24676) datasets were downloaded from Gene Expression Omnibus (GEO) database (https://www.ncbi.nlm.nih.gov/geo/). The GSE26712 dataset was composed of 185 previously untreated late-stage high-grade OC tissue samples and 10 normal ovarian epithelium tissue samples.[9] The GSE23554 dataset contained 28 advanced-stage serous epithelial OC tissue samples with survival information and was applied as validation set.[10] The GSE184880 dataset was a scRNA-seq dataset and included seven treat-naïve high-grade serous OC samples and five age-matched normal ovarian tissue samples.[11]

An extensive collection of RNA modifications-related genes (RMRGs) was gathered from existing literature sources.[12,13] A total of 31 genes derived from m6A, 20 genes derived from m5C,16 genes derived from m1A, 29 genes derived from m7G, 1 gene derived from N4-acetylcytidine (ac4C), 15 genes derived from pseudouracil, 15 genes derived from uridylation, 6 genes derived from A-to-I editing, 2 genes derived from m3C, 3 genes derived from 5-hydroxymethylcytosine (hm5C), 1 gene derived from N6-2'-O-dimethyladenosine (m6Am),3 genes derived from RNA cap methylations, 7 genes derived from 5-methoxycarbonylmethyl-2-thiouridine (mcm5s2U), 14 genes derived from APA and 4 genes derived from RNA ribose methylation. A final 156 genes related to 15 RNA modification patterns were included in this study (Supplementary Table S1).

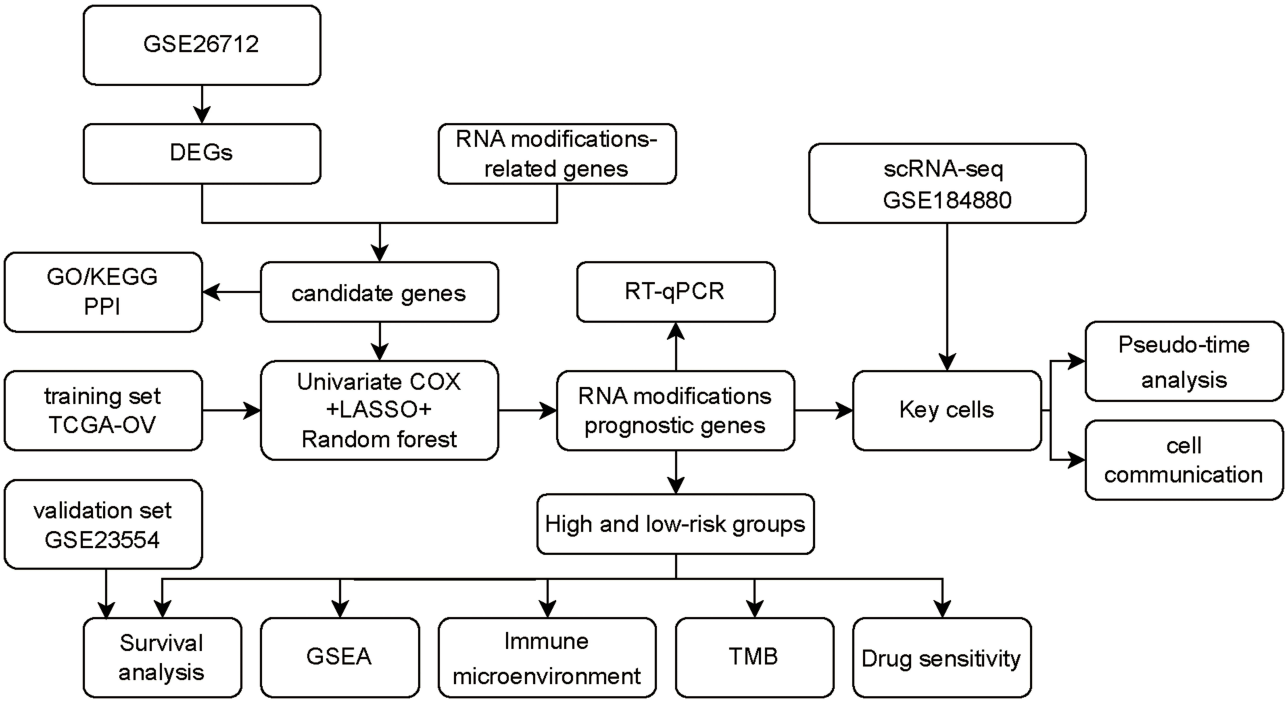

Figure 1 Flowchart of this study.

Identification of Candidate Genes

In GSE26712 dataset, "limma" (v 3.60.6) package was utilized to conduct differential analysis to identify DEGs in OC and control samples ($|\log_2$ FoldChange (FC)$|$ >0.5, adj.p <0.05). In order to attain DEGs related to RNA modifications in OC, "VennDiagram" (v 1.7.3) package was leveraged to take intersection of DEGs and RMRGs to attain candidate genes.

Enrichment Analysis and Protein–Protein Interaction (PPI) Network of Candidate Genes

To explore biological functions and signaling pathways of candidate genes, "clusterProfiler" (v 4.12.6) package was leveraged to perform Gene Ontology (GO) and Kyoto Encyclopedia of Genes and Genomes (KEGG) enrichment analyses on candidate genes ($p < 0.05$). To further understand PPI relationships of proteins encoded by candidate genes, candidate genes were input into Search Tool for Retrieval of Interacting Genes/Proteins (STRING) database (https://cn.string-db.org/) (interaction score ≥0.4) to construct a PPI network. After removing isolated genes, "Cytoscape" (v 3.10.3) software was leveraged to visualize results.

Identification of Prognostic Genes and Construction of Risk Model

In training set, univariate Cox regression analysis (hazard ratio (HR) ≠ 1, $p < 0.2$) was performed on candidate genes via "survival" (v 3.7–0) package. Subsequently, "glmnet" (v 4.1–8) package was utilized to conduct least absolute shrinkage and selection operator (LASSO) regression analysis on prognosis-related genes. After performing 10-fold cross-validation, prognostic genes were attained when gene coefficients were not equal to 0 and lambda (λ) reached minimum.

After the prognostic genes obtained via LASSO regression were standardized in the training set and validation set, "randomForestSRC" (v 3.3.1) package was harnessed to construct a random forest (RF) model (ntree = 100 and mtry = 1).[14] The importance of prognostic genes was demonstrated in line with the RF model, and risk score was calculated. The formula was as follows:

$$\text{RiskScore} = \frac{1}{n}\sum_{i=1}^{n}\text{NodeRiskScore}_i$$

Where n is number of trees in forest, and NodeRiskScore_i is risk score of terminal node where sample is located in the i^{th} tree.

Evaluation and Validation of Risk Model

In training set, in line with the optimal cut-off value of risk score, OC samples were divided into high-risk and low-risk groups. The "ggplot2" (v 3.5.1) package was utilized to draw risk curve plot and survival status plot to display sample distribution. Then, "survival" (v 3.7–0) package was utilized to draw Kaplan–Meier (K-M) curve based on high-risk and low-risk groups, and Log rank test was conducted to examine overall survival (OS) differences between the high-risk and low-risk groups ($p < 0.05$). Meanwhile, "survivalROC" (v 1.0.3.1) package was utilized to draw receiver operating characteristic (ROC) curves for 1 year, 2 years, and 3 years of survival of OC patients to evaluate the effectiveness of risk model (area under curve (AUC) ≥0.6). Finally, the risk model was verified in the validation set pursuant to the above methods.

Gene Set Enrichment Analysis (GSEA)

In training set, to explore the functional enrichment situations in high-risk and low-risk groups, differential analysis on high-risk and low-risk groups was conducted by "DESeq2" (v 1.44.0) package, and $\log_2$ FC was calculated. Then, $\log_2$ FC was sorted in descending order. After that, c2.cp.kegg_legacy.v2024.1.Hs.symbols was attained from Molecular Signatures Database (MSigDB) database (https://www.gsea-msigdb.org/gsea/msigdb) as reference gene set. Subsequently, GSEA enrichment analysis (|Normalized Enrichment Score (NES)| >1, and adj.p <0.05) was performed by "clusterProfiler" (v 4.12.6) package, and top 5 pathways were selected for display pursuant to sorting by adj.p.

Immune Microenvironment and Tumor Mutational Burden (TMB) Analysis

In training set, to examine infiltration status of immune cells in high-risk and low-risk groups, infiltration levels of 28 kinds of immune cells were evaluated by ssGSEA algorithm in "GSVA" (v 2.0.1) package to attain immune scores of each type of immune cell.[15] Furthermore, Wilcoxon rank sum test was conducted by "rstatix" (v 0.7.2) package to compare immune scores of 28 kinds of immune cells in high-risk and low-risk groups, and the differentially immune cells were identified ($p < 0.05$). Box plots were drawn to display the results.

The mutation data of OC patients were downloaded from TCGA database (https://portal.gdc.cancer.gov/). The TMB of each sample was calculated by TMB function of "maftools" (v 2.22.0) package. Waterfall plots of somatic mutations in high-risk and low-risk groups were drawn to display mutation status of 20 genes with the highest mutation rates. Moreover, OC samples were divided into high-TMB and low-TMB groups pursuant to the optimal cut-off value of TMB score via "survival" (v 3.7–0) package. Then, the K-M curves were drawn to judge differences in OS between groups ($p < 0.05$). Then, based on pairwise combinations of high- and low-risk groups and high- and low-TMB groups, including high-risk+high-TMB, high-risk+low-TMB, low-risk+high-TMB, and low-risk+low-TMB groups, K-M curves were drawn to display OS differences among groups.

Chemotherapeutic Drug Sensitivity

In training set, to gain clinical therapeutic drugs for OC, 138 chemotherapeutic drugs were gained from Genomics of Drug Sensitivity in Cancer (GDSC) database (https://www.cancerrxgene.org/), and half-maximal inhibitory concentrations (IC50s) of chemotherapeutic drugs were calculated for each OC sample by "pRRophetic" (v 0.5) package.[16] In addition, IC50 differences of drugs ranging from high-risk and low-risk groups were performed by Wilcoxon test ($p < 0.05$), and top 5 up-regulated and down-regulated drugs were selected for display.

The scRNA-Seq Data Processing

The "Seurat" (v 5.1.0) package was utilized to process scRNA-seq data.[17] The first step was data quality control. The filtering criteria were as follows: each gene was expressed in at least three cells; cells with gene count <200, gene count >7,500, sequence count >30,000, and mitochondrial gene content >20% were excluded. After data was normalized, principal component analysis (PCA) was conducted on the top 2,000 highly variable genes (HVGs). The top 30 principal components (PCs) with statistical significance in the PCA analysis were selected for subsequent analysis. Meanwhile, FindNeighbors and FindClusters functions were employed to identify small cell clusters (threshold: resolution = 0.1). Subsequently, uniform manifold approximation and projection (UMAP) algorithm was utilized to conduct clustering analysis on cell clusters to obtain different cell clusters. Then, to identify screened cell clusters, different cell types were recognized pursuant to marker genes reported in literature.[11]

Identification of Key Cells

In scRNA-seq dataset, based on annotated cells, Wilcoxon test in "rstatix" (v 0.7.2) package was employed to evaluate differential cells in OC and control samples ($p < 0.05$). "ggplot2" (v 3.5.1) package was employed to draw violin plots to display the distribution of prognostic genes in different cells. Subsequently, in each type of cell respectively, Wilcoxon rank sum test in "rstatix" (v 0.7.2) package was conducted to evaluate differences in expression levels of prognosis genes between OC and control samples ($p < 0.05$). Combining expression differences of prognostic genes in identified differential cells between OC and control samples, cells with significant differences in expression of most prognosis genes were selected and defined as key cells.

Pseudo-Time and Cell Communication Analysis

Pseudo-time analysis was performed on key cells to explore their developmental trajectories using "monocle" (v 2.34.0) package.[18] Single-cell trajectory plots were drawn. Next, to detect expression levels of prognosis genes within pseudo-time series, trend plots showing expression levels of prognosis genes within pseudo-time series of key cells were presented. To study potential interactions in OC samples, cell–cell interaction analyses were carried out on annotated cells via "CellChat" (v 2.1.2) package.[19] The number and strength of the cell communication networks were displayed.

Expression and Real-time Quantitative Polymerase Chain Reaction (RT-qPCR) Validation of Prognostic Genes

In GSE26712 dataset, to investigate expression profile of prognostic genes, Wilcoxon rank sum test was performed by "statix" (v 0.7.2) package to examine differential expression levels of prognostic genes between OC and control groups ($p < 0.05$). Boxplots were generated by "ggplot2" (v 3.5.1) package for visualization.

In this study, five pairs of matched OC and tumor-adjacent tissues were acquired from the First Affiliated Hospital of Fujian Medical University. The study was approved by the Ethics Committee of the First Affiliated Hospital of Fujian Medical University and conducted under the guidance of the Declaration of Helsinki. The use of these samples was approved by all patients with the written informed consents. In accordance with the manufacturer's instructions, TRIzol reagent (Ambion, Carlsbad, USA) was utilized to isolate total RNA from tissues. Then, cDNA was generated by reverse transcription using the Hifair®III 1st Strand cDNA synthesis supermix (Yeasen Biotechnology, Shanghai, China). RT-qPCR was performed using the SYBR Green approach (Servicebio, Wuhan, China) in a CFX Connect Real-Time PCR System (Bio-rad, Hercules, USA). GAPDH was used to normalize target gene expression. The relative mRNA expression levels were obtained using the $2^{-\Delta\Delta CT}$ method. The RT-qPCR primer sequences were exhibited in Supplementary Table S2.

Statistical Analysis

In this study, R (v 4.4.1) software was employed for bioinformatics analyses. It was considered that results with a p-value less than 0.05 were statistically significant. The Wilcoxon rank sum test was applied to conduct an analysis of distinctions. RT-qPCR data was evaluated by *t*-test in GraphPad Prism 10 (v 10.1.2) software.

Results

Identification, Functional Enrichment, and PPI Network of RNA Modifications Candidate Genes

A total of 3,891 DEGs were identified between OC group and control group. Among them, 1,853 genes were up-regulated, while 2,038 genes were down-regulated in OC group (adj.p <0.05) (Figure 2A and B). Afterward, intersection of 3,891 DEGs and 156 RMRGs was taken to obtain 34 candidate genes (Figure 2C). Subsequently, results of GO enrichment demonstrated that candidate genes were involved in 268 terms, including 186 biological process (BP) terms such as RNA modification, RNA splicing and regulation of mRNA metabolic process, 37 cellular component (CC) terms such as small nuclear ribonucleoprotein complex, Sm-like protein family complex, and ribonucleoprotein granule, and 45 molecular function (MF) terms such as snRNA binding, catalytic activity, acting on RNA, and mRNA 3'-UTR binding ($p < 0.05$) (Figure 2D). Then, candidate genes were involved in 4 KEGG function pathways, including spliceosome, RNA degradation, mRNA surveillance pathway, and ribosome biogenesis in eukaryotes ($p < 0.05$) (Figure 2E). In addition, among 34 candidate genes, 3 genes had no interactions with others, and proteins encoded by remaining 31 genes had interactions with each other. For example, genes such as *HNRNPA2B1, NCBP2*, and *LSM4* had relatively strong interactions with other genes (Figure 2F).

Construction and Validation of the RNA Modifications-Related Gene Prognostic Model

Univariate Cox regression analysis was used for primary screening of the survival-related genes. The 10 genes (*LSM4, SNRPC, ZC3H13, LSM2, WTAP, FTO, DCP2, PUS7, YTHDC2 and TUT1*) that met the criteria of $p < 0.2$ were retained for further analysis. Among them, 6 genes (*ZC3H13, WTAP, FTO, DCP2, PUS7* and *YTHDC2*) were associated with increased risk with HRs >1, while the other 4 genes (*TUT1, LSM2, LSM4*, and *SNRPC*) were protective genes with HRs <1 (Figure 3A). Then, all 10 genes passed Proportional hazards (PH) test and thus were regarded as prognosis-related genes ($p > 0.05$) (Supplementary Table S3). By performing LASSO Cox regression analysis, according to the λ.min value (λ.min= 0.01476), an eight-gene signature was constructed after integrating 3 genes derived from m6A (*WTAP, ZC3H13*, and *SNRPC*), 1 gene from m7G (*DCP2*), 1 gene from Ψ (*PUS7*), and 3 genes from uridylation (*TUT1, LSM2* and *LSM4*) (Figure 3B and C). Finally, *LSM4, SNRPC, ZC3H13, LSM2, WTAP, DCP2, PUS7*, and *TUT1* were relatively highly important according the RF analysis (Figure 3D).

Based on risk model, OC patients were grouped into high-risk and low-risk groups in accordance with an optimal cut-off value of risk score, which was 80.10132 for training set (High-risk group = 328, low-risk group = 72), 100.7163 for validation set (High-risk group = 9, low-risk group = 19) (Figure 3E). Furthermore, survival status graph demonstrated that a greater risk score corresponded to a larger number of deceased OC samples in training set and validation set (Figure 3F). The K-M curves demonstrated that in training set, p-value was less than 0.0001, and in validation set, p-value was 0.018. A significant difference in survival between high-risk group and low-risk group was observed, and the OS of patients in high-risk group was found to be lower ($p < 0.05$) (Figure 3G). Moreover, in training set, the AUC values of ROC curves for 1 year, 2 years, and 3 years were 0.71, 0.77, and 0.80 respectively, while in validation set, they were 0.82, 0.72, and 0.66, suggesting that risk model possessed a certain level of precision (all AUC ≥ 0.6) (Figure 3H). The above results indicated that a relatively good predictive accuracy for OC patients was achieved by the risk model, and the prognosis of patients in high-risk group was found to be poorer.

GSEA, Comparison of the Immune Activity and TMB Between Subgroups

The results of GSEA demonstrated that a total of 17 pathways were enriched in both high-risk group and low-risk group, such as calcium-signaling pathway, ribosome, oxidative phosphorylation, spliceosome, and so on (Figure 4A and Supplementary Table S4). The results demonstrated that various signaling pathways played a vital function in OC.

The infiltration analysis of 28 kinds of immune cells in high-risk and low-risk groups revealed that immune score of central memory $CD4^+$ T cells was the highest in both risk groups (Figure 4B). A total of 7 differentially immune cells were identified ($p < 0.05$), namely central memory $CD4^+$ T cells, central memory $CD8^+$ T cells, mast cells, memory B cells, neutrophils, plasmacytoid dendritic cells, and regulatory T cells, and their immune scores were all significantly

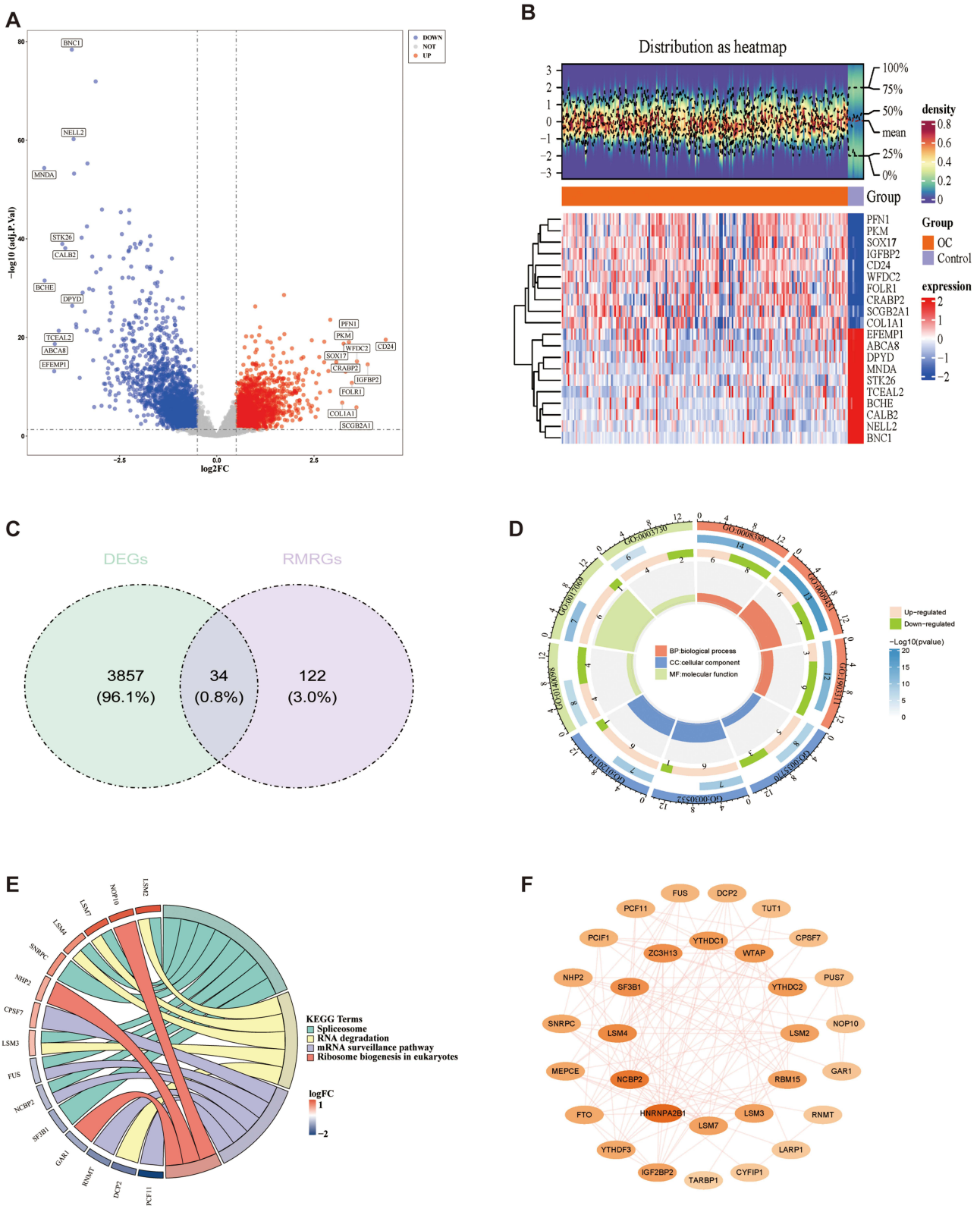

Figure 2 Identification of RNA modifications candidate genes. (**A** and **B**) Volcano diagram and heatmap of DEGs between the OC and control groups in GSE26712 dataset. (**C**) Venn diagram showing the 34 RNA modifications-related genes that were differentially expressed. (**D** and **E**) GO and KEGG analyses of candidate genes. (**F**) PPI network of candidate genes.

https://doi.org/10.2147/IJGM.S523878

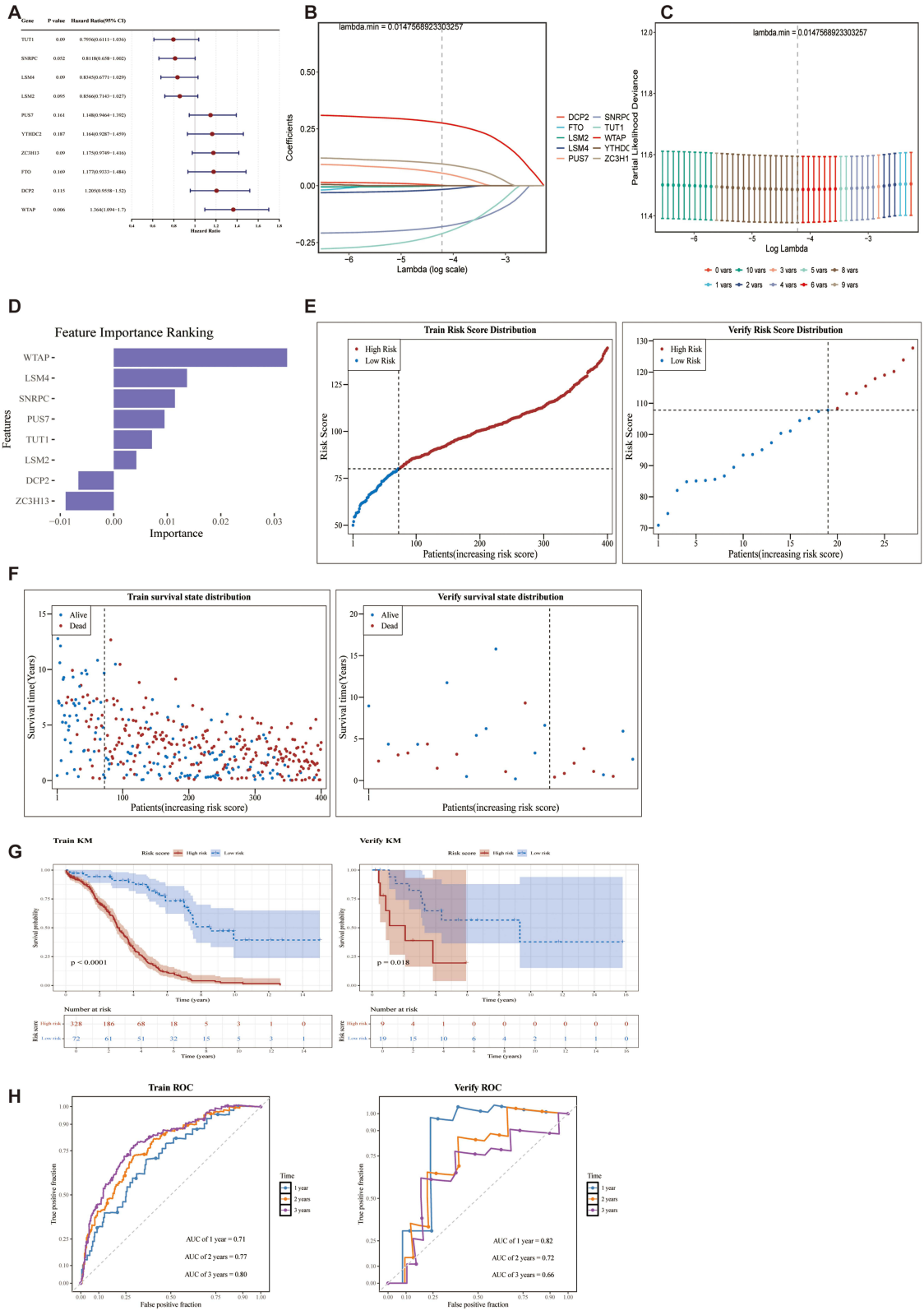

Figure 3 Construction and validation of RNA modifications-related gene prognostic model. (**A**) Univariate Cox regression analysis of OS for each candidate gene. (**B** and **C**) LASSO regression of the 10 prognosis-related genes. (**D**) The importance of prognostic genes by RF analysis. (**E** and **F**) Distribution of the risk score and survival status of patients in the training set and validation set. (**G**) K-M curves of the high-risk and low-risk groups in the training set and validation set. (**H**) ROC curves for predicting 1 year, 2 years and 3 years OS in the training set and validation set.

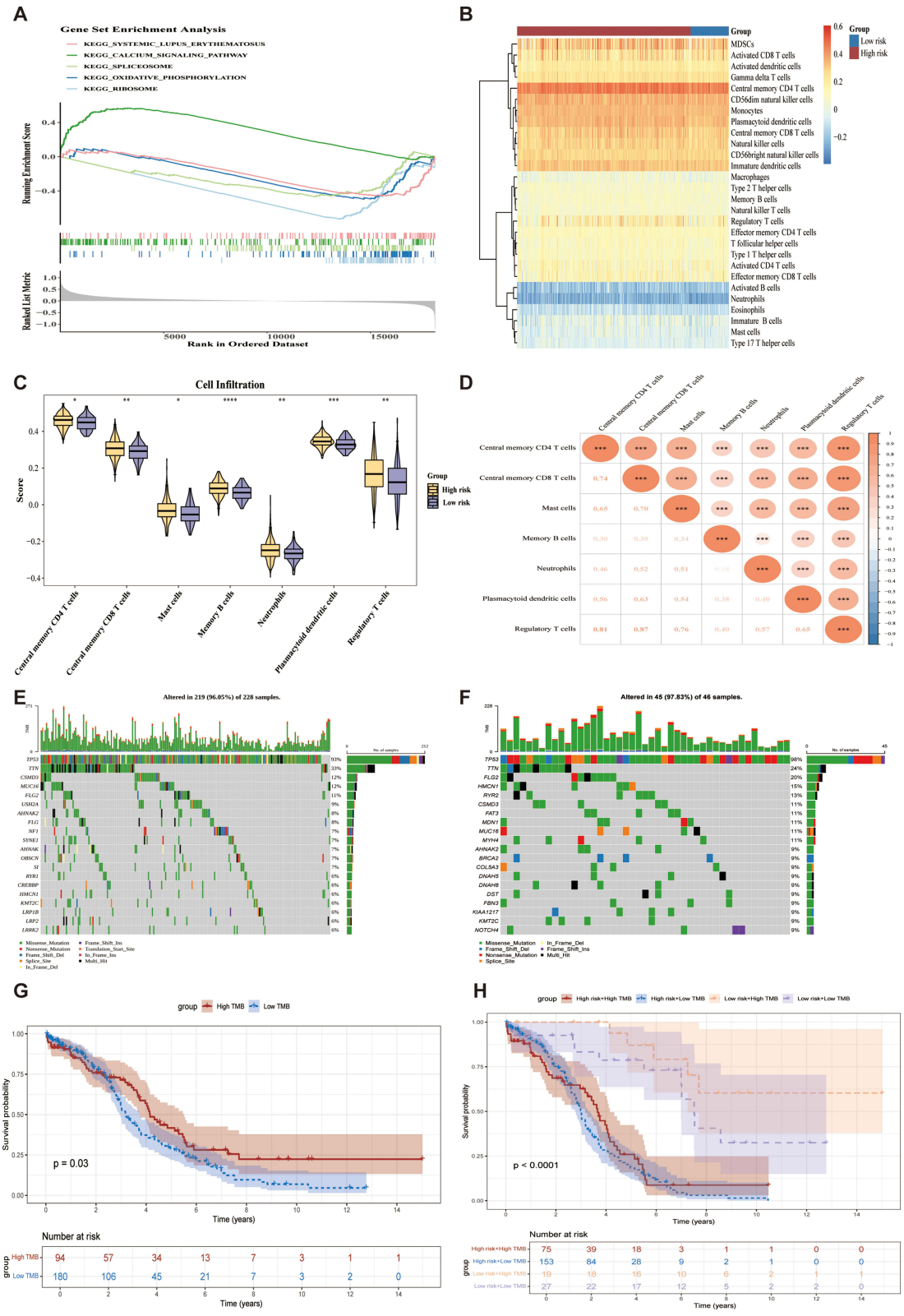

Figure 4 Biological characteristics between high-risk and low-risk groups. (**A**) KEGG enrichment analysis by the GSEA. (**B**) Heatmap showing the 28 immune cells infiltration in the high-risk and low-risk groups. (**C**) Differences in immune cells infiltration between the high-risk and low-risk groups. (**D**) Correlation between differential immune cells in the high-risk and low-risk groups. (**E** and **F**) Waterfall plot highlighting somatic mutations in the high-risk and low-risk groups. (**G**) K-M curves of the high-TMB and low-TMB groups. (**H**) K-M curves of patients stratified by risk score and TMB.

https://doi.org/10.2147/IJGM.S523878

increased in high-risk group (Figure 4C). Moreover, most significant positive connection was observed between regulatory T cells and central memory $CD8^+$ T cells (cor = 0.87, $p < 0.05$) (Figure 4D).

The mutation rates of somatic cells were comparable between the high-risk and low-risk groups, with rates of 96.05% and 97.83%, respectively (Figure 4E and F). The most common mutation type in high-risk and low-risk groups was missense mutation. In high-risk group, 4 genes with the highest mutation numbers were *TP53, TTN, CSMD3*, and *MUC16*, with mutation rates of 93%, 33%, 12%, and 12% respectively. In low-risk group, 3 genes with the highest mutation numbers were *TP53, TTN*, and *FLG2*, with mutation rates of 98%, 24%, and 20% respectively. The OC patients were divided into a high-TMB group with 94 patients and a low-TMB group with 180 patients in accordance with optimal cut-off value of 2.210 for TMB score. Compared with high-TMB group, the OS in low-TMB group was lower ($p = 0.03$) (Figure 4G). The OS of OC patients in high-risk + low-TMB group was lowest when compared with other three groups ($p < 0.0001$) (Figure 4H).

Drug Sensitivity Analysis for Different Risk Groups

Among 138 kinds of drugs, significant differences in IC50 values of 47 drugs were observed in risk groups. A comparative study revealed that the IC50 value of 17 drugs were lower in the low-risk group compared to the high-risk group, such as Paclitaxel, Elesclomol, VX.680, Nutlin.3a and Erlotinib, indicating that the low-risk group was more responsive to these chemotherapy drugs (Figure 5A). Conversely, 30 drugs such as Nilotinib, Embelin, FTI.277, Bleomycin and ABT.263 had significantly lower IC50 levels in the high-risk group than in the low-risk group, suggesting their potential efficacy for the former (Figure 5B).

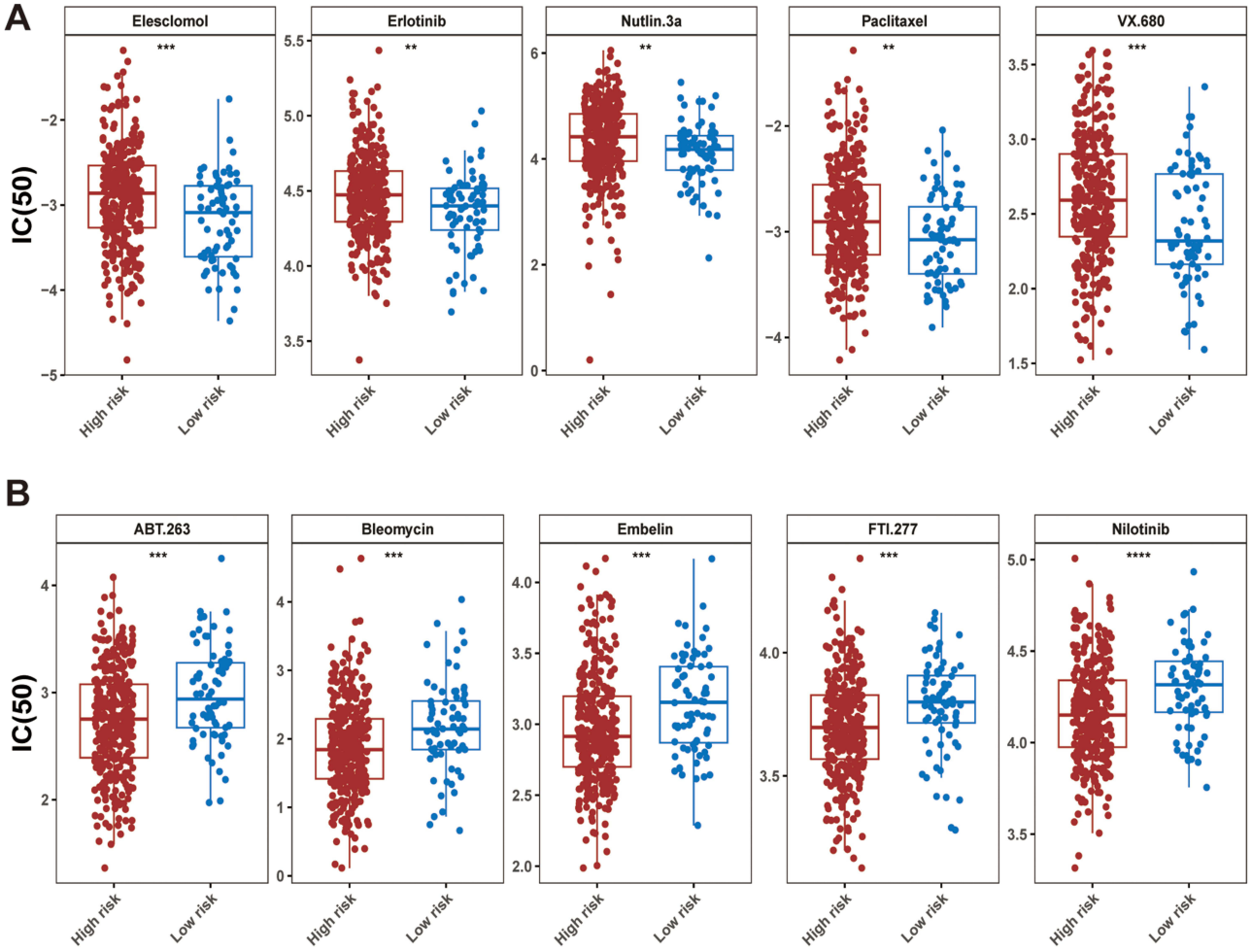

Figure 5 Drug sensitivity analysis of high-risk and low-risk groups. (**A**) The top five significantly different drugs with lower IC50 values in the low-risk group. (**B**) The top five significantly different drugs with lower IC50 values in the high-risk group. **p<0.01, ***p<0.001, ****p<0.0001.

scRNA-Seq Data Analysis and Fibroblast Cells as Key Cells

Before quality control of scRNA-seq data, there were 64,659 cells and 22,334 genes. After quality control, 45,876 cells and 22,334 genes were gained (Supplementary Figure S1A and B). A total of 2000 HVGs were identified such as *IGLC3, IGLC2, IGKC*, etc. (Supplementary Figure S1C). Meanwhile, among 50 PCs, top 30 PCs were selected for analysis ($p < 0.05$) (Supplementary Figure S1D). A total of 16 cell clusters were identified by UMAP clustering analysis (resolution = 0.1) (Figure 6A). Based on the expression of marker genes, cell annotation was performed on different cell clusters, and 8 cell types were gained, including T cells, fibroblast cells, monocytes, endothelial cells, epithelial cells, B/plasma cells, SMC/myofibroblasts, and cell cycle cells (Figure 6B and C). Among them, significant differences between OC group and control group were observed in fibroblast cells, endothelial cells, epithelial cells, B/plasma cells, SMC/myofibroblasts, and cell cycle cells ($p < 0.05$) (Figure 6D). The prognostic genes were mainly distributed in fibroblast cells, epithelial cells and endothelial cells (Figure 6E). In fibroblast cells, significant differences in the expression of *LSM2, LSM4, PUS7, SNRPC, TUT1, WTAP*, and *ZC3H13* between OC group and control group were found (Supplementary Figure S2). Therefore, fibroblast cells were selected as key cells.

Pseudo-Time Analysis and Cell Communications of Fibroblast Cells

Firstly, dimensionality reduction, clustering analyses and cell annotation were performed on fibroblast cells (Supplementary Figure S3). Based on the expression of marker genes,[20,21] fibroblast cells were divided into 5 subpopulations (Figure 7A). Over time, 2 different developmental nodes were presented by fibroblast cells. Compared with other subpopulations, ATRNL1 + KCN + Fib and CXCR4 + CCL5 + Fib cells were more abundant at start of cell development. Fibroblast cells in control group were distributed across all 5 differentiation states, whereas distribution in OC group was significantly reduced in differentiation states 2 and 4. (Figure 7B). Except for *TUT1*, the expression levels of other prognostic genes fluctuated to varying degrees as fibroblast cells differentiated (Figure 7C). In OC group, the most frequent communications were observed between fibroblast cells and endothelial cells, and the strongest communication intensity was found between monocytes and endothelial cells (Figure 7D).

Expression and RT-qPCR Validation of Prognostic Genes

In training set, the prognostic genes demonstrated markedly distinctions between OC and control groups. The expression levels of *LSM2, LSM4, PUS7, SNRPC*, and *TUT1* in OC group were higher than those in control group, while expression levels of *DCP2, WTAP*, and *ZC3H13* in control group were higher than those in the OC group ($p < 0.05$) (Figure 8A). The RT-qPCR results revealed that the expression of *LSM2, LSM4, PUS7, SNRPC*, and *TUT1* were upregulated in OC, while *DCP2, WTAP*, and *ZC3H13* were downregulated. The results of RT-qPCR were consistent with those obtained from the transcriptome dataset, indicating that the identified prognostic genes were reliable (Figure 8B).

Discussion

Ovarian cancer is a highly heterogeneous gynecological malignant tumor characterized by a poor prognosis. Accumulated evidence has showed that RNA modifications can promote or inhibit OC tumorigenesis via regulating cell proliferation, differentiation, invasion, migration, stemness, metabolism, and drug resistance.[5] Understanding the relationship between RNA modifications and OC behavior could provide valuable insights into promising therapeutic targets. Previous studies have been conducted to establish RNA modification gene models with prognostic significance for OC, but they usually focused on a specific RNA modification pattern and ignored the heterogeneity of the tumor.[22,23]

In the present study, we conducted a comprehensive study of multiple RNA modification patterns based on bulk RNA-seq and scRNA-seq data, which was more generally applicable to the evaluation of OC patients. We first identified 34 RNA modifications-related DEGs in OC patients. Via univariate Cox analysis, we obtained 10 genes associated with prognosis in the TCGA dataset. Then LASSO Cox regression model and random survival forest algorithm were combined to screen for the most robust candidate genes. We constructed a prognostic signature consisting of eight RMRGs (*WTAP, ZC3H13, SNRPC, DCP2, PUS7, TUT1, LSM2* and *LSM4*). Compared with previous models that focused on a single RNA modification pattern, our constructed prognostic signature considering multiple RNA modification

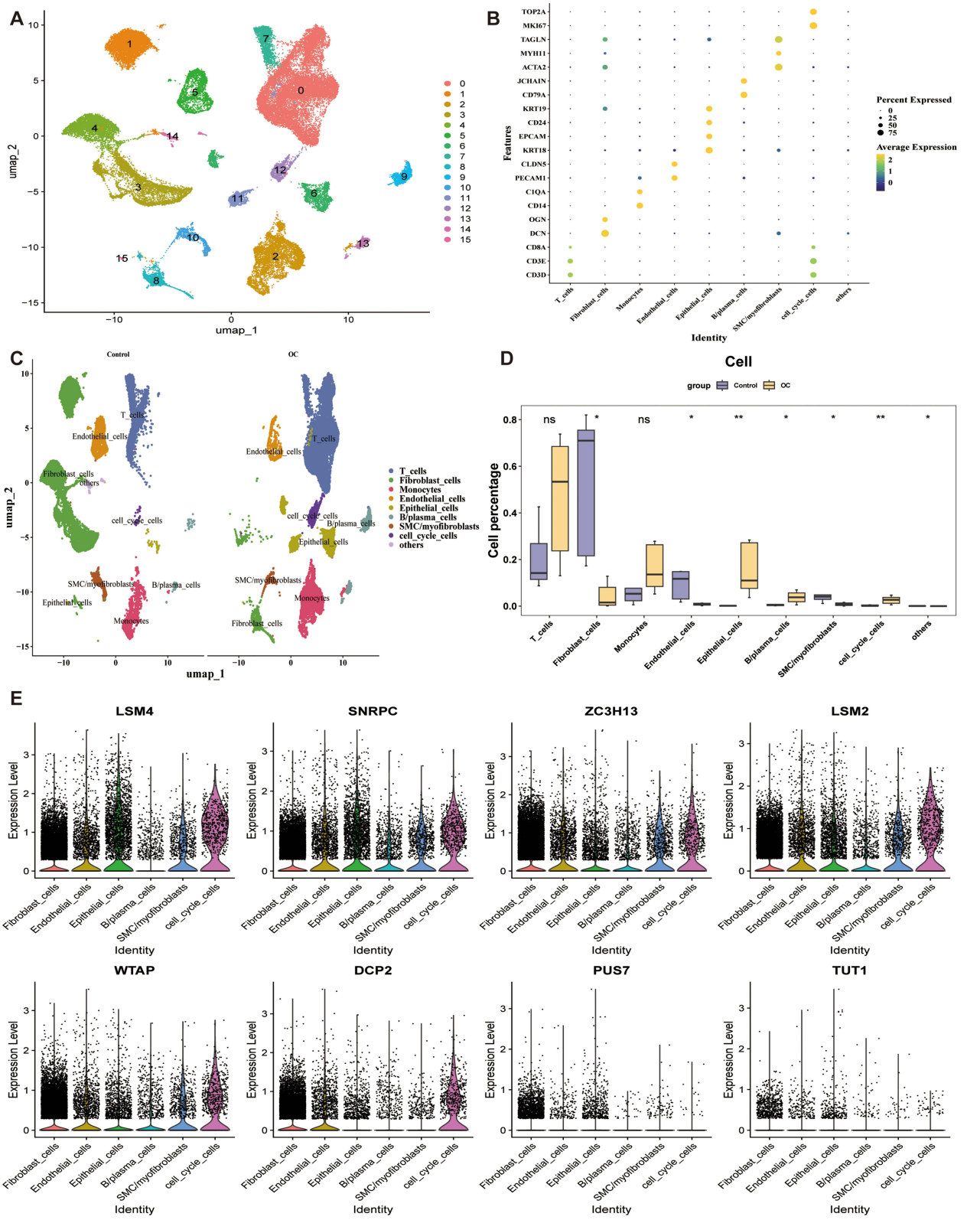

Figure 6 Results of cell clustering and annotation analysis of scRNA-seq data. (**A**) UMAP plot illustrating the distribution and dissimilarity of 16 cell clusters. (**B**) Dot plot showing the expression levels of specific marker genes in each cell type. (**C** and **D**) Proportion of different cell types in OC and control groups. (**E**) The expression of prognostic genes in different cell types. *p<0.05, **p<0.01.

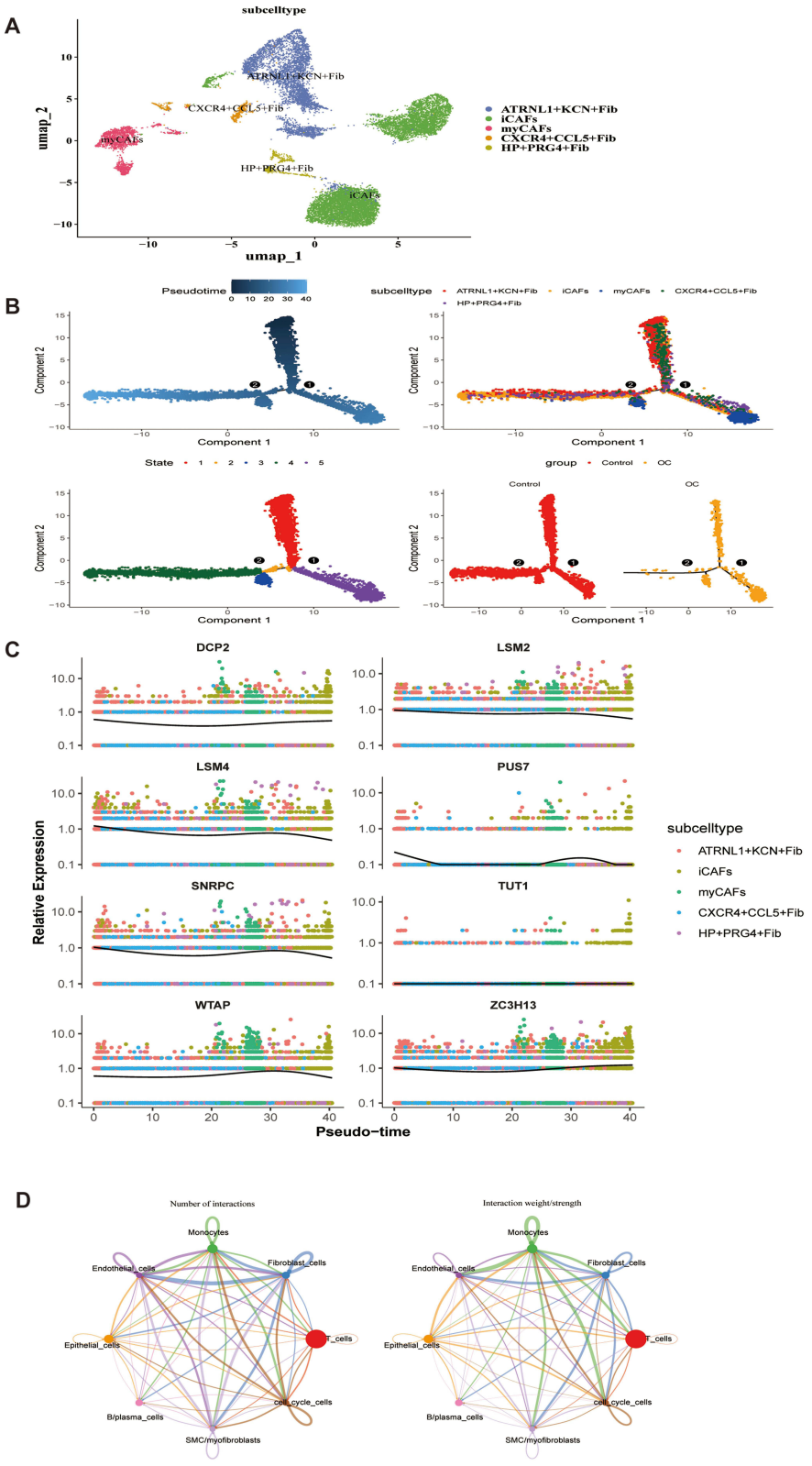

Figure 7 Pseudo-time and cell communication analysis. (**A**) UMAP plot showing that fibroblast cells were clustered into 5 subpopulations. (**B**) Pseudo-time and trajectory analysis of fibroblast cells. (**C**) Expression of prognostic gene in different developmental stages of fibroblast cells. (**D**) Number and strength of interactions between different cells in OC group.

https://doi.org/10.2147/IJGM.S523878

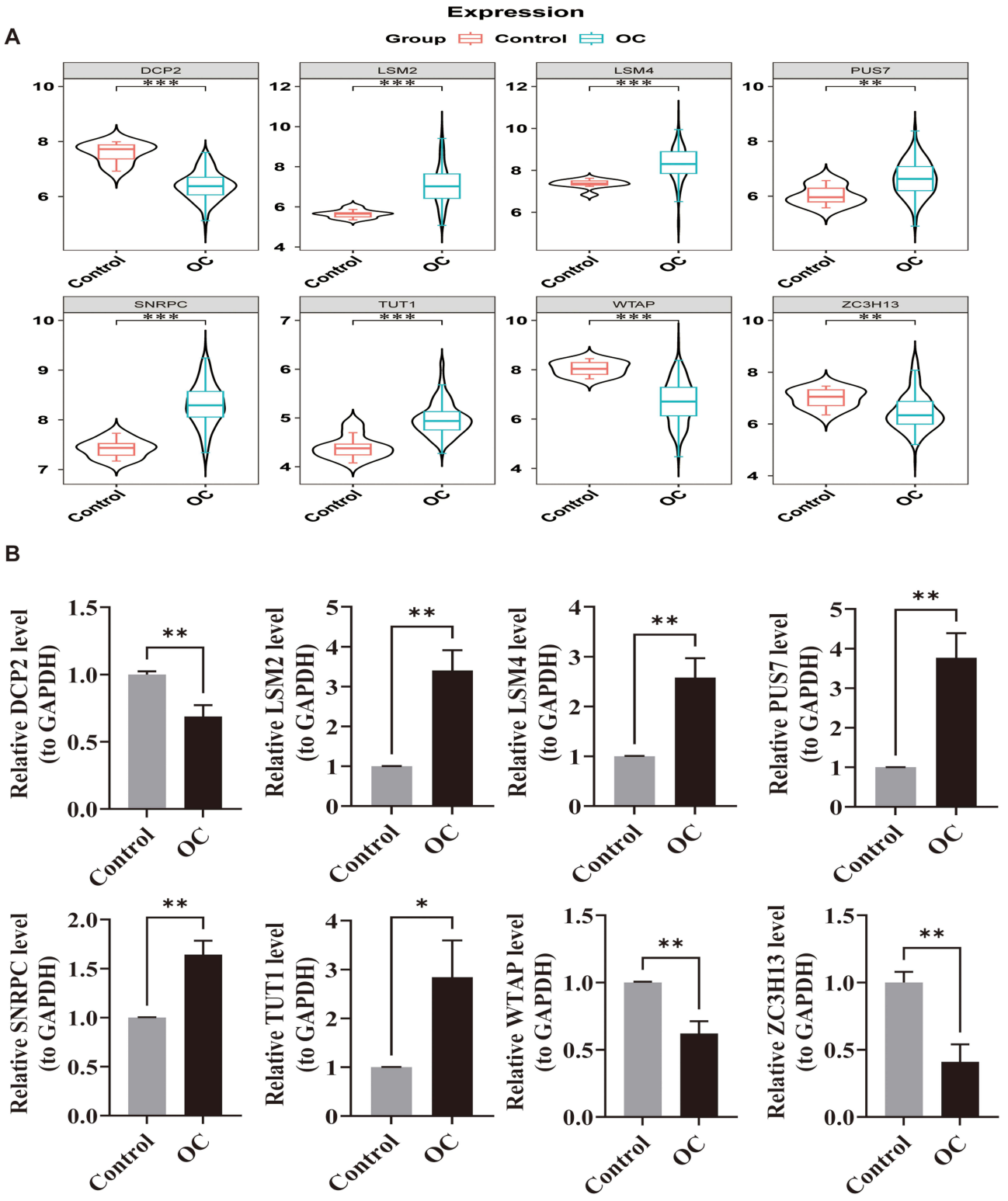

Figure 8 Validation of model gene expression. (**A**) Expression of the prognostic genes between OC and control groups in GSE26712 dataset. (**B**) Verification results of gene expression by RT-qPCR. *p<0.05, **p<0.01, ***p<0.001.

patterns can better capture the complexity of OC and provide a more accurate prediction of prognosis, taking into account the tumor heterogeneity. Based on the optimal cut-off value of risk score, OC patients were divided into high-risk and low-risk groups. The high-risk group exhibited a more unfavorable prognosis. The ROC results confirmed that the model possessed excellent performance in the prognostic prediction of OC, which was further validated in an independent cohort. The RT-qPCR results confirmed that the expression of prognostic genes was consistent with the results of the database, which further verified the true expression of prognostic genes, increasing the credibility of the current study.

Wilms tumor 1-associated protein (WTAP) and zinc finger CCCH domain-containing protein 13 (ZC3H13) are both m6A modification writers. In the present study, these genes were associated with worse prognosis. WTAP, as an m6A modification writer and an oncogene in OC, has been shown to regulate mRNA stability through multiple mechanisms, such as assisting the localization of methyltransferase METTL3-METTL14,[24] binding to the 3'-untranslated region (3' UTR) to improve the stability of mRNA,[25,26] and also influencing miRNA maturation and mitophagy,[27] all of which contribute to OC progression. Overall, the association of WTAP with worse prognosis in our study is consistent with its oncogenic role in OC reported by previous studies, highlighting its potential as a therapeutic target. ZC3H13 is part of an evolutionarily conserved complex.[28] ZC3H13 knockdown can cause a global reduction in m6A modification, especially at the 3' UTR of mRNA.[29] ZC3H13 has been demonstrated to promote chemoresistance in cervical cancer cells via facilitating m6A modification of CENPK mRNA and activating Wnt/β-catenin signaling pathway.[30] However, the role of ZC3H13 in OC has not been fully studied. Our finding that ZC3H13 predicts poor prognosis suggests it may similarly drive OC progression through m6A-dependent pathways, warranting functional validation.

Small nuclear ribonucleoprotein polypeptide C (SNRPC) encodes a subunit of the U1 small nuclear ribonucleoprotein (snRNP) particle, which is required for the splicing process.[31] As a m6A RNA methylation regulator, SNRPC has been demonstrated to promote cell motility by inducing epithelial-mesenchymal transition in hepatocellular carcinoma.[32] Lu et al proved that SNRPC promoted tumor progression by facilitating RNA polymerase II-controlled transcription of oncogenes in breast cancer.[33] However, SNRPC was frequently upregulated, which corresponded to favorable prognosis in patients with OC in our study. This result is consistent with Zhao's research.[34] Therefore, we speculate that the dual roles of SNRPC may stem from tissue-specific RNA splicing targets. In OC, it may stabilize tumor-suppressive transcripts. Given the limited data from OC and the conflicting results in different tumors, further studies are needed to explore the role of *SNRPC* in OC.

Decapping Protein 2 (DCP2) is the major decapping enzyme involved in 5'-3' mRNA decay. DCP2-mediated decapping reaction releases m^7GDP and 5′-monophosphorylated mRNA, which in turn regulates mRNA stability.[35] *DCP2* may be a potential immune-related biomarker which predicts poor prognosis in glioma patients.[36]

Pseudouridine synthase 7 (PUS7) is the only known member of the TruD family which catalyze pseudouridine formation.[37] Emerging evidence suggests that *PUS7* may play a critical role in cancer development. Cui et al demonstrated that *PUS7* promoted glioblastoma tumorigenesis through PUS7-dependent tRNA modification.[38] Zhang et al proved that *PUS7* promoted colorectal cancer cell proliferation by directly stabilizing Sirtuin 1 (SIRT1) and activating the Wnt/β-catenin pathway.[39] Li et al found that *PUS7* was a potential therapeutic target for OC because of its ability to regulate DNA replication and the cell cycle.[40]

Terminal uridylyl transferase 1 (TUT1), Smith-like 2 (LSM2), and Smith-like 4 (LSM4) are uridylation-related genes and may predict good prognosis in the present study. TUT1 conjugates the uridylated-tail to the 3' end of U6 snRNA, providing the binding site of the LSM2-8 complex.[41] In addition, TUT1 functions as a polyadenyltransferase for some specific mRNAs, regulating the oxidative stress response.[42] The LSM protein family is involved in pre-mRNA processing and gene expression regulation.[43] In the nucleus, the LSM2-8 complex functions in pre-mRNA splicing by interacting with U6 snRNA, whereas the LSM1-7 complex functions in mRNA decapping and decay in the cytoplasm.[44]

GO enrichment revealed that the candidate genes were involved in many biological processes, such as RNA splicing and regulation of mRNA metabolic process, which are important in the occurrence and progression of OC. We also carried out functional enrichment in the two risk groups. The results obtained from GSEA revealed that in the high-risk group calcium signaling pathway was activated in the KEGG gene set. Calcium ion (Ca^{2+}) is an important second messenger. Transient receptor potential canonical3 (TRPC3) mediates the transport of Ca^{2+} in plasma membrane and participates in the processes of proliferation, metastasis and invasion in OC.[45] The m6A modification contributes to

TRPC3 mRNA stability, and enhances the malignant behavior of OC cells.[46] In the low-risk group, oxidative phosphorylation pathway was activated. Oxidative phosphorylation plays an important role in the survival and proliferation of ovarian cancer initiating stem cells, and it is also associated with chemotherapeutic resistance of OC.[47] However, it remains to be explored how these pathways are regulated by RNA modification.

The heterogeneity of OC affects the tumor immune microenvironment, and thus affecting the responsiveness of immunotherapy. Therefore, we next investigated the infiltration levels of different immune cells in the two groups. The results revealed that various immune cells, such as regulatory T cells (Tregs), plasmacytoid dendritic cells (pDCs), and central memory T cells, in the high-risk group were significantly more abundant than in the low-risk group. In the TME, the immunosuppressive effect of Tregs may lead to antigenic tolerance of tumor cells, which allows tumor cells to elude immune surveillance and grow.[48] WTAP protein plays a crucial role in the control of activation-induced death of peripheral T cells through enabling Treg cell function.[49] The presence of pDCs is associated with a tolerance phenotype induced by immunosuppressive cytokines or tumor metabolites.[50] Research has found that m6A RNA modifications regulates DC migration.[51] The results showed that the high-risk group had a more immunosuppressive tumor microenvironment, leading to a worse prognosis.

The most common somatic mutation in both high-risk and low-risk groups was *TP53* missense mutation. As a tumor suppressor gene, the mutation in *TP53* results in a loss of the function of cell cycle regulation. Additionally, patients with higher TMB have a higher neoantigen load and are more likely to benefit when receiving immune checkpoint inhibitors therapy. Research has showed that higher TMB was significantly associated with better survival in OC.[52] In the present study, the OC patients in low-risk + high-TMB subgroup had the best prognosis.

Based on the above observations, we further explored differences in sensitivity to chemotherapeutic drugs between the high-risk and low-risk groups. Paclitaxel is commonly used in chemotherapy for OC. The IC50 of paclitaxel in the low-risk group was significantly lower than that in the high-risk group, indicating that the low-risk group displayed better responses to paclitaxel, which also suggested a better prognosis.

Finally, we used scRNA-seq data to provide more sophisticated insights into prognostic gene expression across different cell types. We found that the prognostic genes were mainly distributed in fibroblast cells, epithelial cells and endothelial cells. Especially in the fibroblast cells, there were statistically significant differences in the expression of most prognostic genes between OC and control groups. The ATRNL1 + KCN + Fib subtype was more abundant at the start of fibroblast cell differentiation. This subtype is normal fibroblast which is distributed primarily near cancer cells and has not yet begun to differentiate into cancer-associated fibroblasts (CAFs).[21] As fibroblasts differentiate, CAFs perform critical functions in the TME, where they can promote cancer progression and mediate immune evasion.[53] The expression levels of most prognostic genes fluctuated to varying degrees during fibroblast differentiation. The communication intensity between fibroblast cells and other cells was stronger in OC group. The scRNA-seq results helped us to identify the cell populations at risk.

Nonetheless, our study has some potential limitations. First, the retrospective nature of the TCGA and GEO datasets may introduce confounding factors and inherent biases. In the future, prospective cohorts with larger sample sizes are needed to validate the efficacy of prognostic model. Second, only simple experimental validation was conducted on the prognostic genes, and deeper molecular mechanisms have not been explored. In vitro and in vivo experiments are needed to elucidate the exact functional mechanisms of RMRGs in OC progression. Therefore, translating the prognostic model into clinical applications still requires a comprehensive assessment.

Conclusion

In conclusion, our study has developed an RNA modifications-related prognostic signature that is effective in predicting clinical outcomes and therapeutic responses in patients with OC. Our comprehensive analysis of RNA modifications may contribute to the understanding of the TME and provide new insights into the field of OC research.

Abbreviations

AUC, Area under curve; BP, Biological process; CC, Cellular component; DEG, Differentially expressed gene; FC, FoldChange; GEO, Gene Expression Omnibus; GO, Gene Ontology; GSEA, Gene set enrichment analysis; HVGs,

Highly variable genes; IC50, Half-maximal inhibitory concentration; KEGG, Kyoto Encyclopedia of Genes and Genomes; K-M, Kaplan-Meier; LASSO, Least absolute shrinkage and selection operator; MF, Molecular function; OC, Ovarian cancer; OS, Overall survival; PCA, Principal component analysis; PCs, Principal components; PH, Proportional hazards; PPI, protein–protein interaction; RF, Random forest; RMRGs, RNA modifications-related genes; ROC, Receiver operating characteristic; RT-qPCR, real-time quantitative polymerase chain reaction; scRNA-seq, Single-cell RNA sequencing; TCGA, The Cancer Genome Atlas; TMB, Tumor mutational burden; TME, Tumor microenvironment; UMAP, Uniform manifold approximation and projection.

Ethical Approval

This study obtained the approval of the Ethics Committee of the First Affiliated Hospital of Fujian Medical University and conducted under the guidance of the Declaration of Helsinki. The patients had signed an informed consent form.

Acknowledgments

We are very grateful for the data provided by the TCGA and GEO observation databases.

Author Contributions

All authors made a significant contribution to the work reported, whether that is in the conception, study design, execution, acquisition of data, analysis and interpretation, or in all these areas; took part in drafting, revising or critically reviewing the article; gave final approval of the version to be published; have agreed on the journal to which the article has been submitted; and agree to be accountable for all aspects of the work.

Funding

This research was supported by the Research Fund from the Education Department of Fujian Province (JAT200155).

Disclosure

The authors declare that they have no competing interests.

References

1. Konstantinopoulos PA, Matulonis UA. Clinical and translational advances in ovarian cancer therapy. *Nat Cancer*. 2023;4(9):1239–1257. doi:10.1038/s43018-023-00617-9
2. Kopper O, de Witte CJ, Lõhmussaar K, et al. An organoid platform for ovarian cancer captures intra- and interpatient heterogeneity. *Nat Med*. 2019;25(5):838–849. doi:10.1038/s41591-019-0422-6
3. Bose S, Saha P, Chatterjee B, Srivastava AK. Chemokines driven ovarian cancer progression, metastasis and chemoresistance: potential pharmacological targets for cancer therapy. *Semin Cancer Biol*. 2022;86(Pt 2):568–579. doi:10.1016/j.semcancer.2022.03.028
4. Boccaletto P, Stefaniak F, Ray A, et al. MODOMICS: a database of RNA modification pathways. 2021 update. *Nucleic Acids Res*. 2022;50(D1): D231–D5. doi:10.1093/nar/gkab1083
5. Tang Q, Li L, Wang Y, et al. RNA modifications in cancer. *Br J Cancer*. 2023;129(2):204–221. doi:10.1038/s41416-023-02275-1
6. Bi X, Lv X, Liu D, et al. METTL3-mediated maturation of miR-126-5p promotes ovarian cancer progression via PTEN-mediated PI3K/Akt/mTOR pathway. *Cancer Gene Ther*. 2021;28(3–4):335–349.
7. Liu X, Wei Q, Yang C, et al. RNA m5C modification upregulates E2F1 expression in a manner dependent on YBX1 phase separation and promotes tumor progression in ovarian cancer. *Exp Mol Med*. 2024;56(3):600–615.
8. Zhang Y, Wang D, Peng M, et al. Single-cell RNA sequencing in cancer research. *J Exp Clin Cancer Res*. 2021;40(1):81.
9. Bonome T, Levine DA, Shih J, et al. A gene signature predicting for survival in suboptimally debulked patients with ovarian cancer. *Cancer Res*. 2008;68(13):5478–5486.
10. Marchion DC, Cottrill HM, Xiong Y, et al. BAD phosphorylation determines ovarian cancer chemosensitivity and patient survival. *Clin Cancer Res*. 2011;17(19):6356–6366. doi:10.1158/1078-0432.CCR-11-0735
11. Xu J, Fang Y, Chen K, et al. Single-cell RNA sequencing reveals the tissue architecture in human high-grade serous ovarian cancer. *Clin Cancer Res*. 2022;28(16):3590–3602. doi:10.1158/1078-0432.CCR-22-0296
12. Cui L, Ma R, Cai J, et al. RNA modifications: importance in immune cell biology and related diseases. *Signal Transduct Target Ther*. 2022;7 (1):334. doi:10.1038/s41392-022-01175-9
13. Luo Y, Tian W, Kang D, et al. RNA modification gene WDR4 facilitates tumor progression and immunotherapy resistance in breast cancer. *J Adv Res*. 2024. doi:10.1016/j.jare.2024.06.029
14. Wang H, Zhou L. Random survival forest with space extensions for censored data. *Artif Intell Med*. 2017;79:52–61. doi:10.1016/j.artmed.2017.06.005

15. Charoentong P, Finotello F, Angelova M, et al. Pan-cancer immunogenomic analyses reveal genotype-immunophenotype relationships and predictors of response to checkpoint blockade. *Cell Rep*. 2017;18(1):248–262. doi:10.1016/j.celrep.2016.12.019
16. Geeleher P, Cox N, Huang RS. pRRophetic: an R package for prediction of clinical chemotherapeutic response from tumor gene expression levels. *PLoS One*. 2014;9(9):e107468. doi:10.1371/journal.pone.0107468
17. Satija R, Farrell JA, Gennert D, Schier AF, Regev A. Spatial reconstruction of single-cell gene expression data. *Nat Biotechnol*. 2015;33(5):495–502. doi:10.1038/nbt.3192
18. Trapnell C, Cacchiarelli D, Grimsby J, et al. The dynamics and regulators of cell fate decisions are revealed by pseudotemporal ordering of single cells. *Nat Biotechnol*. 2014;32(4):381–386. doi:10.1038/nbt.2859
19. Luo J, Deng M, Zhang X, Sun X. ESICCC as a systematic computational framework for evaluation, selection, and integration of cell-cell communication inference methods. *Genome Res*. 2023;33(10):1788–1805. doi:10.1101/gr.278001.123
20. Yang D, Liu J, Qian H, Zhuang Q. Cancer-associated fibroblasts: from basic science to anticancer therapy. *Exp Mol Med*. 2023;55(7):1322–1332. doi:10.1038/s12276-023-01013-0
21. Ding B, Ye Z, Yin H, et al. Comprehensive single-cell analysis reveals heterogeneity of fibroblast subpopulations in ovarian cancer tissue microenvironment. *Heliyon*. 2024;10(6):e27873. doi:10.1016/j.heliyon.2024.e27873
22. Tan W, Liu S, Deng Z, et al. Gene signature of m6A-related targets to predict prognosis and immunotherapy response in ovarian cancer. *J Cancer Res Clin Oncol*. 2023;149(2):593–608. doi:10.1007/s00432-022-04162-3
23. Liu J, Chen C, Wang Y, et al. Comprehensive of N1-methyladenosine modifications patterns and immunological characteristics in ovarian cancer. *Front Immunol*. 2021;12:746647. doi:10.3389/fimmu.2021.746647
24. Ping X-L, Sun B-F, Wang L, et al. Mammalian WTAP is a regulatory subunit of the RNA N6-methyladenosine methyltransferase. *Cell Res*. 2014;24(2):177–189. doi:10.1038/cr.2014.3
25. Tang J, Wang F, Cheng G, et al. Wilms' tumor 1-associating protein promotes renal cell carcinoma proliferation by regulating CDK2 mRNA stability. *J Exp Clin Cancer Res*. 2018;37(1):40. doi:10.1186/s13046-018-0706-6
26. Wang J, Zheng F, Wang D, Yang Q. Regulation of ULK1 by WTAP/IGF2BP3 axis enhances mitophagy and progression in epithelial ovarian cancer. *Cell Death Dis*. 2024;15(1):97. doi:10.1038/s41419-024-06477-0
27. Lyu Y, Zhang Y, Wang Y, et al. HIF-1α regulated WTAP overexpression promoting the Warburg effect of ovarian cancer by m6a-dependent manner. *J Immunol Res*. 2022;2022:6130806. doi:10.1155/2022/6130806
28. Wen J, Lv R, Ma H, et al. Zc3h13 regulates nuclear RNA m6A methylation and mouse embryonic stem cell self-renewal. *Mol Cell*. 2018;69(6):1028–1038.e6. doi:10.1016/j.molcel.2018.02.015
29. Knuckles P, Lence T, Haussmann IU, et al. Zc3h13/Flacc is required for adenosine methylation by bridging the mRNA-binding factor Rbm15/Spenito to the m6A machinery component Wtap/Fl(2)d. *Genes Dev*. 2018;32(5–6):415–429. doi:10.1101/gad.309146.117
30. Lin X, Wang F, Chen J, et al. N6-methyladenosine modification of CENPK mRNA by ZC3H13 promotes cervical cancer stemness and chemoresistance. *Mil Med Res*. 2022;9(1):19. doi:10.1186/s40779-022-00378-z
31. Libri D, Duconge F, Levy L, Vinauger M. A role for the Psi-U mismatch in the recognition of the 5' splice site of yeast introns by the U1 small nuclear ribonucleoprotein particle. *J Biol Chem*. 2002;277(20):18173–18181. doi:10.1074/jbc.M112460200
32. Zhang Y, Qiu J, Zuo D, et al. SNRPC promotes hepatocellular carcinoma cell motility by inducing epithelial-mesenchymal transition. *FEBS Open Bio*. 2021;11(6):1757–1770. doi:10.1002/2211-5463.13175
33. Lu -X-X, Yang W-X, Pei Y-C, et al. An in vivo CRISPR screen identifies that SNRPC promotes triple-negative breast cancer progression. *Cancer Res*. 2023;83(12):2000–2015. doi:10.1158/0008-5472.CAN-22-0536
34. Zhao L, Tang Y, Yang J, et al. Integrative analysis of circadian clock with prognostic and immunological biomarker identification in ovarian cancer. *Front Mol Biosci*. 2023;10:1208132. doi:10.3389/fmolb.2023.1208132
35. Wurm JP, Sprangers R. Dcp2: an mRNA decapping enzyme that adopts many different shapes and forms. *Curr Opin Struct Biol*. 2019;59:115–123. doi:10.1016/j.sbi.2019.07.009
36. Mei Y, Lv Q, Tan Z, et al. Decapping enzyme 2 is a novel immune-related biomarker that predicts poor prognosis in glioma. *Biotechnol Genet Eng Rev*. 2024;40(4):4262–4283. doi:10.1080/02648725.2023.2209409
37. Rintala-Dempsey AC, Kothe U. Eukaryotic stand-alone pseudouridine synthases - RNA modifying enzymes and emerging regulators of gene expression? *RNA Biol*. 2017;14(9):1185–1196. doi:10.1080/15476286.2016.1276150
38. Cui Q, Yin K, Zhang X, et al. Targeting PUS7 suppresses tRNA pseudouridylation and glioblastoma tumorigenesis. *Nat Cancer*. 2021;2(9):932–949. doi:10.1038/s43018-021-00238-0
39. Zhang Q, Fei S, Zhao Y, et al. PUS7 promotes the proliferation of colorectal cancer cells by directly stabilizing SIRT1 to activate the Wnt/β-catenin pathway. *Mol, Carcinog*. 2023;62(2):160–173. doi:10.1002/mc.23473
40. Li H, Chen L, Han Y, et al. The identification of RNA modification gene PUS7 as a potential biomarker of ovarian cancer. *Biology*. 2021;10(11).
41. Kim J, Tsuruta F, Okajima T, Yano S, Sato B, Chiba T. KLHL7 promotes TUT1 ubiquitination associated with nucleolar integrity: implications for retinitis pigmentosa. *Biochem Biophys Res Commun*. 2017;494(1–2):220–226. doi:10.1016/j.bbrc.2017.10.049
42. Mellman DL, Gonzales ML, Song C, et al. A PtdIns4,5P2-regulated nuclear poly(A) polymerase controls expression of select mRNAs. *Nature*. 2008;451(7181):1013–1017. doi:10.1038/nature06666
43. Lekontseva NV, Stolboushkina EA, Nikulin AD. Diversity of LSM family proteins: similarities and differences. *Biochemistry*. 2021;86(Suppl 1):S38–S49. doi:10.1134/S0006297921140042
44. Spiller MP, Reijns MAM, Beggs JD. Requirements for nuclear localization of the Lsm2-8p complex and competition between nuclear and cytoplasmic Lsm complexes. *J Cell Sci*. 2007;120(Pt 24):4310–4320. doi:10.1242/jcs.019943
45. Deng F, Fu M, Zhao C, et al. Calcium signals and potential therapy targets in ovarian cancer. *Int J Oncol*. 2023;63(5). doi:10.3892/ijo.2023.5573.
46. Shen Z, Gu L, Liu Y, et al. PLAA suppresses ovarian cancer metastasis via METTL3-mediated m6A modification of TRPC3 mRNA. *Oncogene*. 2022;41(35):4145–4158. doi:10.1038/s41388-022-02411-w
47. Wu Y, Zhang X, Wang Z, Zheng W, Cao H, Shen W. Targeting oxidative phosphorylation as an approach for the treatment of ovarian cancer. *Front Oncol*. 2022;12:971479. doi:10.3389/fonc.2022.971479
48. Wang Z-B, Zhang X, Fang C, et al. Immunotherapy and the ovarian cancer microenvironment: exploring potential strategies for enhanced treatment efficacy. *Immunology*. 2024;173(1):14–32. doi:10.1111/imm.13793

49. Ito-Kureha T, Leoni C, Borland K, et al. The function of Wtap in N6-adenosine methylation of mRNAs controls T cell receptor signaling and survival of T cells. *Nat Immunol*. 2022;23(8):1208–1221. doi:10.1038/s41590-022-01268-1
50. Monti M, Ferrari G, Gazzurelli L, Bugatti M, Facchetti F, Vermi W. Plasmacytoid dendritic cells at the forefront of anti-cancer immunity: rewiring strategies for tumor microenvironment remodeling. *J Exp Clin Cancer Res*. 2024;43(1):196.
51. Kong Y, Yu J, Ge S, Fan X. Novel insight into RNA modifications in tumor immunity: promising targets to prevent tumor immune escape. *Innovation* 2023;4(4):100452. doi:10.1016/j.xinn.2023.100452
52. Fan S, Gao X, Qin Q, Li H, Yuan Z, Zhao S. Association between tumor mutation burden and immune infiltration in ovarian cancer. *Int Immunopharmacol*. 2020;89(Pt A):107126. doi:10.1016/j.intimp.2020.107126
53. Lavie D, Ben-Shmuel A, Erez N, Scherz-Shouval R. Cancer-associated fibroblasts in the single-cell era. *Nat Cancer*. 2022;3(7):793–807.